Published in final edited form as:
J Immunol. 2005 August 1; 175(3): 1851–1857.

A Shared Epitope of the Interphotoreceptor Retinoid-Binding Protein Recognized by the CD4+ and CD8+ Autoreactive T Cells[1]

Hui Shao, **Yong Peng**, **Tianjiang Liao**, **Meiqin Wang**, **Ming Song**, **Henry J. Kaplan**, and **Deming Sun**[2]
Department of Ophthalmology and Visual Sciences, Kentucky Lions Eye Center, University of Louisville, Louisville, KY 40202

Abstract

We previously demonstrated that cultures of rat uveitogenic T cells rapidly become dominated by $CD4^+$ cells, but activation of $CD8^+$ autoreactive T cells also occurred during the in vitro culture of in vivo-primed T cells. In the present study, we show that the commonly used uveitogenic peptide, interphotoreceptor retinoid-binding protein (IRBP) 1–20, generated both $CD4^+$ and $CD8^+$ autoreactive T cells in the C57BL/6 (B6) mouse and that this 20-mer contains at least two distinct antigenic epitopes. To determine whether the CD8 response was Ag-specific and whether $CD4^+$ and $CD8^+$ IRBP1–20-specific T cells recognize distinct antigenic epitopes, we prepared highly purified $CD4^+$ and $CD8^+$ T cells from IRBP1–20-primed mice and tested their proliferative response to a large panel of truncated peptides derived from IRBP1–20. The results showed that both $CD4^+$ and $CD8^+$ T cells recognized the same spectrum of peptides. In addition, peptides P10–18 were found to bind effectively to $CD8^+$ IRBP1–20-specific T cells when complexed with recombinant H-$2K^b$ and also stimulate the proliferation and cytokine production of $CD4^+$ IRBP1–20-specific T cells. Our results document for the first time that $CD8^+$ and $CD4^+$ autoreactive T cells display characteristic epitope recognition and they both recognize the same core epitope.

Uveitis is a common cause of human visual disability and blindness. Recurrent uveitis is associated with severe clinical complications, such as cystoid macular edema, cataract formation, and glaucoma. Experimental models have been generated in rodents by immunization with several different ocular Ags, one of which, interphotoreceptor retinoid-binding protein (IRBP),[3] has been widely studied in mice (1–3).

[1]This work was supported in part by National Institutes of Health Grants NEI EY12974 (to H.S.), EY14599 (to H.S.), and NEI EY014366 (to D.S.), Grant RG3413A4 from the National Multiple Sclerosis Society, the Commonwealth of Kentucky Research Challenge Trust Fund, and Research to Prevent Blindness (New York, NY). H.S. is a recipient of a career development award from Research to Prevent Blindness.

[2] Address correspondence and reprint requests to Dr. Deming Sun, Department of Ophthalmology and Vision Sciences, Kentucky Lions Eye Center, University of Louisville, 301 East Muhammad Ali Boulevard, Louisville, KY 40202. d0sun001@louisville.edu.

Disclosures
The authors have no financial conflict of interest.

[3]Abbreviations used in this paper: IRBP, interphotoreceptor retinoid-binding protein; EAU, experimental autoimmune uveitis; p.i., postimmunization; EAE, experimental autoimmune encephalitis.

Early studies found that uveitogenic T cells in either the mouse or rat were predominantly $CD4^+$ (4–6); however, we recently demonstrated that the uveitogenic T cells induced in the Lewis rat by immunization with a synthetic IRBP-derived peptide, IRBP1177–1191, consisted of both $CD4^+$ and $CD8^+$ T cells (7). Therefore, we examined the situation in a mouse model of uveitis. We first used the CSFE staining technique (7–10) to examine the Ag-specific proliferation and/or expansion of in vivo-primed $CD8^+$ IRBP1–20-specific T cells. Because typical antigenic epitopes for $CD8^+$ T cells consist of 9–10 aa (11, 12), we also determined the minimal antigenic epitope required for the activation of CD4 and CD8 T cell subsets by measuring the stimulatory activity of truncated peptides covering the whole length of IRBP1–20 on $CD4^+$ and $CD8^+$ IRBP1–20-specific T cells and the binding to $CD8^+$ IRBP1–20-specific T cells of these peptides in the form of a complex with recombinant MHC class I ($H\text{-}2K^b$) molecules. The results showed that both the CD4 and $CD8^+$ autoreactive T cells recognized the same core epitope.

Materials and Methods

Animals and reagents

Pathogen-free female C57BL/6 mice (8–10 wk old) were purchased from The Jackson Laboratory and were housed and maintained in the animal facilities of the University of Louisville. Institutional approval was obtained and institutional guidelines regarding animal experimentation followed.

The sequences of IRBP 1–20 and the truncated peptides are listed in Table I. All were synthesized by Pepscan Systems and were >85% pure.

Abs against mouse $H\text{-}2D^b$ (KH95), mouse $H\text{-}2K^b$ (AF6-88), and mouse $H\text{-}2K^b/H\text{-}2D^b$ mAbs were obtained from BioLegend.

Animal model of experimental autoimmune uveitis (EAU)

Briefly, to prepare T cells, donor mice were immunized s.c. with 200 μl of an emulsion containing 200 μg of IRBP1–20 and 500 μg of *Mycobacterium tuberculosis* H37Ra (Difco) in IFA (Sigma-Aldrich), distributed over six spots on the tail base and flank. Uveitis was induced in naive B6 mice by adoptive transfer of 5×10^6 IRBP1–20-specific T cells as described previously (13–15). The animals were examined three times a week for clinical signs of uveitis by fundoscopy, starting at the second week post-transfer. Fundoscopic evaluation for longitudinal follow-up of disease was performed using a binocular microscope after pupil dilation using 0.5% tropicamide and 1.25% phenylephrine hydrochloride ophthalmic solutions. The incidence and severity of EAU were graded on a scale of 0–4 in half-point increments using the criteria described previously (16), which are based on the type, number, and size of lesions present.

Pathological examination

Inflammation in the eye was confirmed by histopathology. Whole eyes were collected, immersed for 1 h in 4% phosphate-buffered glutaraldehyde, and transferred to 10% phosphate-buffered formaldehyde until processed. The fixed and dehydrated tissue was

embedded in methacrylate, and 5-μm sections were cut through the pupillary-optic nerve plane and stained with H&E. The presence or absence of disease was evaluated blind by examining six sections cut at different levels for each eye. Severity of EAU was scored on a scale of 0 (no disease) to 4 (maximum disease) in half-point increments, as described previously (15).

IRBP1–20-specific T cells

T cells from IRBP1–20-immunized B6 mice were isolated 13 days postimmunization (p.i.) from lymph node cells or spleen cells by passage through a nylon wool column, then 1×10^7 cells in 2 ml of RPMI 1640 medium in a 6-well plate (Costar) were stimulated with 20 μg/ml IRBP1–20 in the presence of 1×10^7 irradiated syngeneic spleen cells as APCs. After 2 days, the activated lymphoblasts were isolated by gradient centrifugation on Lymphoprep (Robbins Scientific) and cultured in RPMI 1640 medium supplemented with 15% IL-2-containing medium (supernatant form Con A-stimulated rat spleen cells).

Proliferation assay

T cells from IRBP1–20-immunized B6 mice were prepared and seeded at 4×10^5 cells per well in 96-well plates, then cultured at 37°C for 48 h in a total volume of 200 μl of medium with or without IRBP-derived peptides in the presence of irradiated (2000 rad) syngeneic spleen APCs (2×10^5), and [^{3}H]thymidine incorporation during the last 8 h was assessed using a microplate scintillation counter (Packard). The proliferative response was expressed as the mean cpm ± SD of triplicate determinations.

Purification of CD4$^+$ and CD8$^+$ T cells using StemSep columns

CD4$^+$ and CD8$^+$-enriched T cell populations were isolated from freshly prepared draining lymph node and spleen cells using negative selection StemSep kits (Stem Cell Technology). The mouse lymph node and spleen cells were incubated with mixtures of bispecific Ab complexes, each of which binds both to dextran beads and to CD4 or CD8 and to a cell surface Ag on mouse hemopoietic cells (CD11b; Mac-1), NK cells (DX5), B cells (CD45R; B220), erythroid cells (TER119), or polymorphonuclear leukocytes (Ly-6G; Gr-1). The cells were then incubated for 15 min at 4°C with StemSep Magnetic Colloid, loaded into a magnetic column, and washed with 15 ml of medium according to the manufacturer's protocol. The flow-through fraction containing either CD4$^+$ or CD8$^+$-enriched cells was collected, and the purity of the isolated cell fraction was determined by flow cytometry using FITC-conjugated anti-TCR Abs and PE-conjugated anti-CD4 or anti-CD8 Abs.

CFSE staining

T cells from the draining lymph nodes and spleen from immunized mice were prepared by passage through a nylon wool column and stained with the vital dye, CFSE (Molecular Probes) as described previously (8). Briefly, the cells were washed and resuspended at 50×10^6 cells/ml in serum-free RPMI 1640 medium, then incubated at 37°C for 10 min with gentle shaking with a final concentration of 10 μM CFSE, washed twice with and resuspended in RPMI 1640 medium containing 10% FCS, stimulated with peptides and irradiated APCs, and analyzed by flow cytometry.

Flow cytometric detection of T cells binding IRBP peptides complexed with recombinant MHC class I (H-2K^b) dimers

The MHC class I (H-2K^b) molecule used was a fusion protein containing mouse H-2K^b and mouse IgG1 obtained from BD Pharmingen (17). To produce the dimeric form, it was incubated at 4°C for 12–24 h with human β_2-microglobulin (both at a final concentration of 0.15 mg/ml) and an excess of the test peptide (1 mg/ml). Double staining was performed by incubating 5×10^5 cells with 0.5 μg of peptide-dimer complexes at 4°C for 30 min in a volume of 0.5 ml. The cells were washed twice in PBS containing 1% BSA and 0.1% sodium azide and stained with a PE-labeled anti-mouse IgG1 Ab, followed by a FITC-conjugated Ab against either CD4 or CD8. The results are presented as PE staining vs FITC staining.

Immunofluorescence flow cytometry

Aliquots of 2×10^5 cells were double-stained with combinations of FITC-or PE-conjugated mAbs against mouse $\alpha\beta$TCR (H57), CD4, or CD8. All Abs were purchased from BD Biosciences. Data collection and analysis were performed on a FACSCalibur flow cytometer using CellQuest software.

Statistical analysis

The data are expressed as the mean ± SD. Each experiment was repeated at least three times.

Results

Detection of CD8$^+$ IRBP1–20-specific T cells using CFSE staining

In a previous study, we demonstrated that, although cultures of rat uveitogenic T cells are predominantly CD4$^+$ cells, culture of the in vivo-primed lymphocytes also contains significant numbers of CD8$^+$ autoreactive T cells (7). To further characterize these CD8$^+$ autoreactive T cells and determine their role in the pathogenesis of mouse EAU, we immunized B6 mice with IRBP1–20, a known uveitogenic peptide derived from IRBP (3, 18), then prepared T cells from these mice at day 13 p.i. and labeled them with CFSE before stimulation with IRBP1–20 in the presence of irradiated syngeneic APCs (spleen cells). The activated T cell blasts were then separated by Ficoll gradient centrifugation, cultured in IL-2-containing medium, stained with PE-labeled anti-CD4 or anti-CD8 Abs, and subjected to FACS analysis. As shown in Fig. 1*A*, at 96–120 h after in vitro activation, ~40% of the IRBP1–20-specific T cells expressed CD8. This T cell response was Ag-specific, as a specificity test (Fig. 1*B*) showed that a strong response was only seen using the immunizing peptide.

Response of in vivo IRBP1–20-primed T cells to truncated IRBP peptides

Because IRBP1–20 used for immunization contains 20 aa residues, we examined whether this 20-mer peptide contained separate antigenic epitope(s) stimulating either CD4$^+$ or CD8$^+$ T cells using a panel of 24 truncated peptides derived from IRBP1–20 (Table I) by truncation of the N and/or C terminus, including the peptide FQPSLVLDM (P6–14) which was predicted to contain the best “CD8-stimulating motif” by a computer program (Peptide

Binding Predictions programs ⟨http://bimas.dcrt.nih.gov/molbio/hla_bind⟩). To assess the response of $CD8^+$ and $CD4^+$ T cells separately, we isolated $CD8^+$ and $CD4^+$ T cells from the spleen of IRBP1–20-immunized mice using StemSep columns.

The purity of the $CD4^+$ and $CD8^+$ T cells was verified by staining with FITC-labeled Abs followed by FACS analysis (Fig. 2*A*), then their proliferative responses to the truncated peptides were determined. A representative proliferation result (Fig. 2*B*) shows that the peptide IRBP1–20 and many of the truncated peptides had a strong stimulatory effect on both $CD8^+$ and $CD4^+$ T cells. Although the purified $CD8^+$ T cells had a generally lower response to the test peptides than the $CD4^+$ T cells, it is apparent that the response of $CD8^+$ T cells is not always CD4-dependent. A further group of peptides was tested (Fig. 3), and the results showed that truncated peptides P2–20, P3–20, and P4–20 were as effective as P1–20 in stimulating both CD4 and CD8 T cells (Fig. 3*A*), indicating that the first three N-terminal residues were not essential. Similarly, the C-terminal residues 15–20 were also functionally redundant in terms of stimulating both sets of T cells (Fig. 3*B*). Removal of residue 14[M] (P3–13) resulted in no loss of ability to stimulate CD4 cells, but in a 50% decrease in the CD8 cell response, indicating that residue 15 is more important for the CD8 response. In summary, none of the truncated peptides stimulated only CD4 or CD8 T cells.

The short peptide P10–18 was also found to stimulate both a CD4 and a CD8 T cell response (Fig. 3*C*). Interestingly, addition of 1–3 residues to the N terminus (residues 9, 8, and 7) almost totally abolished this effect (Fig. 3*C*). Because P3–13 and P10–18 overlap each other by only four amino acids (residues 10–13) and the sequence of the peptides are significantly different, we hypothesize that IRBP1–20 contains at least two separate T cell activation epitopes. Interestingly, the 9-mer peptide, P6–14 (FQPSLVLDM), which was predicted by a computer program to have the highest potential for binding to MHC class I (H-$2D^b$ and H-$2K^b$) molecules, had no appreciable stimulatory effect on CD8 cells (Fig. 2*A*) and did not bind to the recombinant H-$2K^b$ molecule (see Fig. 5).

The response of $CD8^+$ IRBP1–20-specific T cells to P10–18 is H-2D/K^b-restricted

From the shortest peptides that still activated T cells, we choose P10–18 for more intensive study. To determine whether the response to this peptide was restricted by K^b or D^b of the MHC class I molecules, we performed an Ab-blocking test in which $CD8^+$ T cells purified from IRBP1–20-immunized mice 13 days p.i. using a StemSep column were exposed to P10–18 in the presence of syngeneic APCs in the presence or absence of class I blocking Abs. As shown in Fig. 4, the response to P10–18 was partially blocked by Abs specific for H-$2K^b$ or D^b, even though anti-K^b Abs blocked more consistently; a complete block can be seen when Abs reactive both D^b and K^b were applied.

Binding to $CD8^+$ IRBP1–20-specific T cells of MHC class I (H-$2K^b$) molecules complexed with P10–18

We then examined the binding of complexes of recombinant H-$2K^b$ dimers and truncated IRBP peptides to IRBP1–20-specific $CD8^+$ T cells. Nylon wool-enriched splenic T cells from mice immunized with IRBP1–20 were stimulated with IRBP1–20 and expanded in IL-2-containing medium for 5–7 days, then were incubated with the recombinant H-$2K^b$

molecule complexed with various truncated peptides, and double-stained with FITC-labeled anti-mouse CD8 Ab and a PE-labeled Ab detecting bound complex (see *Materials and Methods*). Fig. 5 shows that the percentage of CD8 IRBP-expanded T cells bound to complexed H-2K^b molecules depended on the peptide in the complex. The greatest binding of H-2K^b molecules was seen using peptide P10–18, which bound to 29% of the cells, whereas the 20-mer peptide P1–20 showed lower, but significant, binding (9.5% of the cells). The binding assay was absolutely peptide-dependent; for example, addition of a single amino acid to the C terminus of P10–18 (P10–19) or to the N terminus (P9–18) almost totally abolished binding activity. Parallel studies showed that the binding activity of the peptide did not correlate with the T cell stimulatory effect of the peptide; for example, peptide P1–20 maximally stimulated the proliferative response of both CD4 and CD8$^+$ IRBP1–20-specific T cells, but bound only to a low percentage of CD8$^+$ T cells. It is noted that staining of P1–20-specific T cells with P10–18 and K^b-fusion protein reveals that a small portion of the binding cells are CD8-negative. This might be due to a part of the newly activated CD8 cells that has down-regulated CD8 expression, even though they retain the expression of TCR after a new stimulation.

Adoptive transfer of disease by P10–18- and P3–13-activated IRBP1–20-specific T cells

To determine whether P10–18- and P3–13-activated IRBP1–20-specific T cells had uveitis-inducing capability, T cells from IRBP1–20-immunized B6 mice were separately stimulated in vitro with IRBP1–20, P10–18, or P3–13, and the activated T cell blasts were transferred to naive B6 recipients. As shown in Fig. 6, comparable disease severity, examined by either fundoscopy or histology, was comparable all three groups of mice.

Discussion

Autoimmune diseases, such as experimental autoimmune encephalitis (EAE) and EAU, have been believed to be mainly caused by CD4$^+$ autoreactive T cells. This conclusion was supported by the observation that established encephalitogenic T cell lines, such as MBP-specific (19) or proteolipid protein-specific (20, 21) encephalitogenic lines and IRBP-specific (4) or retinal-soluble Ag-specific (5, 6) uveitogenic T cells, are exclusively CD4$^+$$\alpha\beta$TCR$^+$. Upon transfer to syngeneic naive animals, these CD4$^+$ autoreactive T cell lines are capable of causing the related autoimmune disease (4–6).

However, a pathogenic role of autoreactive CD8$^+$ T cells has been demonstrated in a number of autoimmune diseases, such as diabetes (22, 23), arthritis (24), and proteolipid protein-induced EAE (25) in the mouse. In the study of EAE, other laboratories (26–28) and our own (17, 29) have demonstrated that CD8$^+$ encephalitogenic T cells play a major role in MOG-induced EAE in the B6 mouse. Our recent studies have also shown that coactivation of CD8$^+$ uveitogenic T cells can be readily demonstrated in IRBP-induced uveitis in the rat (7). We have also found, using the CSFE staining technique, that uveitogenic IRBP-specific T cells in the mouse also contain CD8$^+$ T cells (Fig. 1).

To determine whether the activation of CD4 and CD8 autore-active T cells is driven by separate antigenic epitopes within IRBP1–20, we synthesized a panel of truncated peptides covering the length of IRBP1–20 and tested their stimulatory activity on CD4 and CD8 T

cells. The results showed that highly purified $CD8^+$ T cells from B6 mice primed in vivo with IRBP1–20 responded significantly to IRBP1–20 and its truncated peptides in the absence of CD4 help (Fig. 2); however, the response of the purified CD8 cells was much weaker than that of their CD4 counterparts, but could be greatly enhanced by adding nanogram per milliliter concentrations of cytokines, such as IL-2 and IL-7 (data not shown).

Our initial experimental goal was to determine whether the 20-mer IRBP1–20 contained separate CD4 and CD8 T cell epitopes. However, repeated assays on a large panel of truncated peptides failed to identify a peptide that stimulated only $CD8^+$ or $CD4^+$ T cells. Based on the observations that two of the shortest peptides, P3–13 and P10–18, retained the ability to stimulate $CD4^+$ and $CD8^+$ IRBP1–20-specific T cells and that the response of purified CD8 cells was more effectively blocked by anti-H-$2K^b$ Abs than anti-H-$2D^b$ Abs, we assessed their binding to recombinant H-$2K^b$ molecules. The results showed that ~30% of the proliferating $CD8^+$ T cells bound H-$2K^b$ molecules conjugated to P10–18. The fact that P10–18 effectively stimulated and bound to $CD8^+$ IRBP-specific T cells after forming a complex with recombinant H-$2K^b$ molecules while being able to stimulate highly purified $CD4^+$ T cells strongly suggest that this peptide binds both to MHC class I and class II molecules and is recognized by $CD4^+$ and $CD8^+$ IRBP-specific autoreactive T cells.

A typical $CD8^+$ T cell antigenic epitope is composed of 9–10 aa (11, 12); however, in our study, many IRBP peptides longer than 9-mers (up to 13-mers) had CD8 stimulatory activity. It has also been recently demonstrated that peptides can fit into the MHC class I groove by inserting both ends into the groove, leaving the rest of the peptide as a “bulge” outside the groove (30, 31). It is also worth mentioning that peptide P6–14, a candidate peptide predicted to bind H-$2D^b$ and H-$2K^b$ MHC I molecules by computer software (Peptide Binding Predictions programs ⟨http:// bimas.dcrt.nih.gov/molbio/hla_bind⟩), totally failed to stimulate $CD8^+$ T cells and did not bind to recombinant H-$2K^b$.

To determine whether a single epitope was able to stimulate both $CD4^+$ and $CD8^+$ autoreactive T cells in other systems, we recently re-examined a panel of truncated peptides derived from MOG35–55, an encephalitogenic epitope in the B6 mouse (17, 29), and found that highly purified $CD4^+$ and $CD8^+$ T cells from MOG35–55-primed B6 mice also respond to the same epitope within this peptide (our unpublished results).

We found that there was not always a correlation between the stimulatory and binding activity of an IRBP peptide. For example, IRBP1–20 and most of the truncated peptides larger that 14-mers had a stimulatory activity on CD8 activation; however, strong binding to peptide-complexed MHC I molecules was only seen with peptides P10–18 and P3–13. One possible explanation is that, in the proliferation assay or in vivo, serum or cellular proteases might further cleave and process the longer peptides to fit the MHC binding groove, whereas, in the absence of APCs, only those peptides that already fit the MHC groove can bind.

In conclusion, our results demonstrate, for the first time, that, unlike the T cell response to viral proteins in which $CD8^+$ T cells recognize different antigenic epitopes compared with

their $CD4^+$ T cell counterparts, $CD4^+$ and $CD8^+$ IRBP1–20-specific autore-active T cells recognize the same antigenic epitope(s).

Acknowledgments

We greatly appreciate the helpful discussion of Drs. Jack Bennink and Darcy Wilson and the editorial assistance of Dr. Tom Barkas.

References

1. Fox GM, Kuwabara T, Wiggert B, Redmond TM, Hess HH, Chader GJ, Gery I. Experimental autoimmune uveoretinitis (EAU) induced by retinal interphotoreceptor retinoid-binding protein (IRBP): differences between EAU induced by IRBP and by S-antigen. Clin. Immunol. Immunopathol. 1987; 43:256–264. [PubMed: 3494559]
2. Silver PB, Rizzo LV, Chan CC, Donoso LA, Wiggert B, Caspi RR. Identification of a major pathogenic epitope in the human IRBP molecule recognized by mice of the $H\text{-}2^r$ haplotype. Invest. Ophthalmol. Vis. Sci. 1995; 36:946–954. [PubMed: 7706044]
3. Avichezer D, Silver PB, Chan CC, Wiggert B, Caspi RR. Identification of a new epitope of human IRBP that induces autoimmune uveoretinitis in mice of the $H\text{-}2^b$ haplotype. Invest. Ophthalmol. Vis. Sci. 2000; 41:127–131. [PubMed: 10634611]
4. Rizzo LV, Silver P, Wiggert B, Hakim F, Gazzinelli RT, Chan CC, Caspi RR. Establishment and characterization of a murine $CD4^+$ T cell line and clone that induce experimental autoimmune uveoretinitis in B10.A mice. J. Immunol. 1996; 156:1654–1660. [PubMed: 8568272]
5. Rozenszajn LA, Muellenberg-Coulombre C, Gery I, El-Saied M, Kuwabara T, Mochizuki M, Lando Z, Nussenblatt RB. Induction of experimental autoimmune uveoretinitis by T-cell lines. Immunology. 1986; 57:559–565. [PubMed: 3485569]
6. Gregerson DS, Obritsch WF, Fling SP, Cameron JD. S-antigen-specific rat T cell lines recognize peptide fragments of S-antigen and mediate experimental autoimmune uveoretinitis and pinealitis. J. Immunol. 1986; 136:2875–2882. [PubMed: 2420873]
7. Shao H, Sun SL, Kaplan HJ, Sun D. Characterization of rat $CD8^+$ uveitogenic T cells specific for interphotoreceptor retinal-binding protein 1177–1191. J. Immunol. 2004; 173:2849–2854. [PubMed: 15295004]
8. Lyons AB, Parish CR. Determination of lymphocyte division by flow cytometry. J. Immunol. Methods. 1994; 171:131–137. [PubMed: 8176234]
9. Lyons AB. Analysing cell division in vivo and in vitro using flow cytometric measurement of CFSE dye dilution. J. Immunol. Methods. 2000; 243:147–154. [PubMed: 10986412]
10. Tang Q, Henriksen KJ, Boden EK, Tooley AJ, Ye J, Subudhi SK, Zheng XX, Strom TB, Bluestone JA. Cutting edge: CD28 controls peripheral homeostasis of $CD4^+CD25^+$ regulatory T cells. J. Immunol. 2003; 171:3348–3352. [PubMed: 14500627]
11. Rötzschke O, Falk K, Deres K, Schild H, Norda M, Metzger J, Jung G, Rammensee HG. Isolation and analysis of naturally processed viral peptides as recognized by cytotoxic T cells. Nature. 1990; 348:252–254. [PubMed: 1700304]
12. Rammensee HG, Falk K, Rötzschke O. Peptides naturally presented by MHC class I molecules. Annu.Rev. Immunol. 1993; 11:213–244.
13. Shao H, Lei S, Sun S, Xiang J, Kaplan HJ, Sun D. CpGODN1826 converts the weak uveitogenic rat IRBP1181–91 peptide into a strong uveitogen. J. Immunol. 2003; 171:4780–4785. [PubMed: 14568955]
14. Shao H, Song L, Sun SL, Kaplan HJ, Sun D. Conversion of monophasic to recurrent autoimmune disease by autoreactive T cell subsets. J. Immunol. 2003; 171:5624–5630. [PubMed: 14607971]
15. Shao H, Fu Y-X, Song L, Sun S, Kaplan HJ, Sun D. LTβR-Ig treatment blocks actively induced, but not adoptively transferred, uveitis in Lewis rats. Eur. J. Immunol. 2003; 33:1743.
16. Thurau SR, Chan CC, Nussenblatt RB, Caspi RR. Oral tolerance in a murine model of relapsing experimental autoimmune uveoretinitis (EAU): induction of protective tolerance in primed animals. Clin. Exp. Immunol. 1997; 109:370–376. [PubMed: 9276535]

17. Sun D, Zhang Y, Wei B, Peiper SC, Shao H, Kaplan HJ. Encephalitogenic activity of truncated myelin oligodendrocyte glycoprotein (MOG) peptides and their recognition by $CD8^+$ MOG-specific T cells on oligomeric MHC class I molecules. Int. Immunol. 2003; 15:261–268. [PubMed: 12578856]

18. Avichezer D, Liou GI, Chan CC, Lewis GM, Wiggert B, Donoso LA, Nickerson JM, Crawford MA, Caspi RR. Interphotoreceptor retinoid-binding protein (IRBP)-deficient C57BL/6 mice have enhanced immunological and immunopathogenic responses to IRBP and an altered recognition of IRBP epitopes. J. Autoimmun. 2003; 21:185–194. [PubMed: 14599843]

19. Sun D, Qin Y, Chluba J, Epplen JT, Wekerle H. Suppression of experimentally-induced autoimmune encephalomyelitis by cytolytic T-T cell interactions. Nature. 1988; 332:843–846. [PubMed: 2965794]

20. Tuohy VK, Lu Z, Sobel RA, Laursen RA, Lees MB. A synthetic peptide from myelin proteolipid protein induces experimental allergic encephalomyelitis. J. Immunol. 1988; 141:1126–1130. [PubMed: 2456341]

21. Reddy J, Bettelli E, Nicholson L, Waldner H, Jang MH, Wucherpfennig KW, Kuchroo VK. Detection of autoreactive myelin proteolipid protein 139–151-specific T cells by using MHC II (IAs) tetramers. J. Immunol. 2003; 170:870–877. [PubMed: 12517952]

22. Wang B, Gonzalez A, Benoist C, Mathis D. The role of $CD8^+$ T cells in the initiation of insulin-dependent diabetes mellitus. Eur. J. Immunol. 1996; 26:1762–1769. [PubMed: 8765018]

23. Nagata M, Santamaria P, Kawamura T, Utsugi T, Yoon JW. Evidence for the role of $CD8^+$ cytotoxic T cells in the destruction of pancreatic β-cells in nonobese diabetic mice. J. Immunol. 1994; 152:2042–2050. [PubMed: 7907110]

24. Tada Y, Ho A, Koh DR, Mak TW. Collagen-induced arthritis in CD4- or CD8-deficient mice—$CD8^+$ T cells play a role in initiation and regulate recovery phase of collagen-induced arthritis. J. Immunol. 1996; 156:4520–4526. [PubMed: 8666829]

25. Biddison WE, Cruikshank WW, Center DM, Pelfrey CM, Taub DD, Turner RV. $CD8^+$ myelin peptide-specific T cells can chemoattract $CD4^+$ myelin peptide-specific T cells: importance of IFN-inducible protein 10. J. Immunol. 1998; 160:444–448. [PubMed: 9552002]

26. Perchellet A, Stromnes I, Pang JM, Goverman J. CD8+ T cells maintain tolerance to myelin basic protein by “epitope theft”. Nat. Immunol. 2004; 5:606–614. [PubMed: 15146180]

27. Huseby ES, Liggitt D, Brabb T, Schnabel B, Ohlen C, Goverman J. A pathogenic role for myelin-specific $CD8^+$ T cells in a model for multiple sclerosis. J. Exp. Med. 2001; 194:669–676. [PubMed: 11535634]

28. Zeng R, Spolski R, Finkelstein SE, Oh S, Kovanen PE, Hinrichs CS, Pise-Masison CA, Radonovich MF, Brady JN, Restifo NP, et al. Synergy of IL-21 and IL-15 in regulating $CD8^+$ T cell expansion and function. J. Exp. Med. 2005; 201:139–148. [PubMed: 15630141]

29. Sun D, Whitaker JN, Huang Z, Liu D, Coleclough C, Wekerle H, Raine CS. Myelin antigen-specific $CD8^+$ T cells are encephalitogenic and produce severe disease in C57BL/6 mice. J. Immunol. 2001; 166:7579–7587. [PubMed: 11390514]

30. Macdonald WA, Purcell AW, Mifsud NA, Ely LK, Williams DS, Chang L, Gorman JJ, Clements CS, Kjer-Nielsen L, Koelle DM, et al. A naturally selected dimorphism within the HLA-B44 supertype alters class I structure, peptide repertoire, and T cell recognition. J. Exp. Med. 2003; 198:679–691. [PubMed: 12939341]

31. Zernich D, Purcell AW, Macdonald WA, Kjer-Nielsen L, Ely LK, Laham N, Crockford T, Mifsud NA, Bharadwaj M, Chang L, et al. Natural HLA class I polymorphism controls the pathway of antigen presentation and susceptibility to viral evasion. J. Exp. Med. 2004; 200:13–24. [PubMed: 15226359]

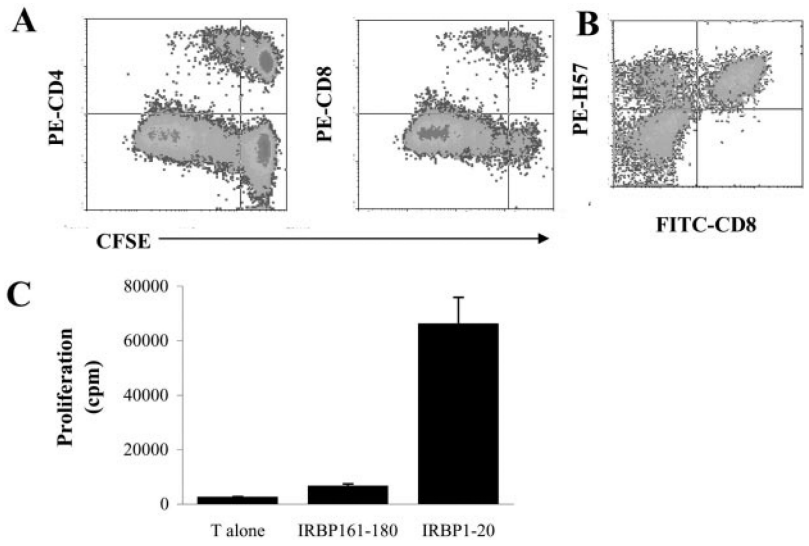

FIGURE 1.

Detection of CD8$^+$ IRBP1–20-specific T cells using CFSE staining. *A*, Nylon wool-enriched T cells, prepared from IRBP1–20-immunized B6 mice 13 days p.i., were stained with CFSE, then stimulated with IRBP1–20 and APCs, and the activated T cell blasts separated on a Ficoll gradient and recultured in IL-2-containing medium for 2–3 days. For FACS analysis, the T cells were stained with PE-labeled Abs against mouse CD4 or CD8. *B*, Nylon wool-enriched T cells, prepared from IRBP1–20-immunized B6 mice 13 days p.i., were stimulated with IRBP1–20 and APCs. The activated T cell blasts were separated on a Ficoll gradient, recultured in IL-2-containing medium for 2–3 days, and dually stained with PE-anti-mouse TCR (H57) and FITC-anti-mouse CD8. *C*, Specificity of the T cell proliferative response to IRBP1–20. Nylon wool-enriched T cells from IRBP1–20-immunized B6 mice were cultured at 37°C for 48 h in 96-well microtiter plates with syngeneic APC with or without IRBP1–20, and [^{3}H]thymidine incorporation during the last 8 h was assessed. The proliferative response is expressed as the mean cpm ± SD for triplicate wells.

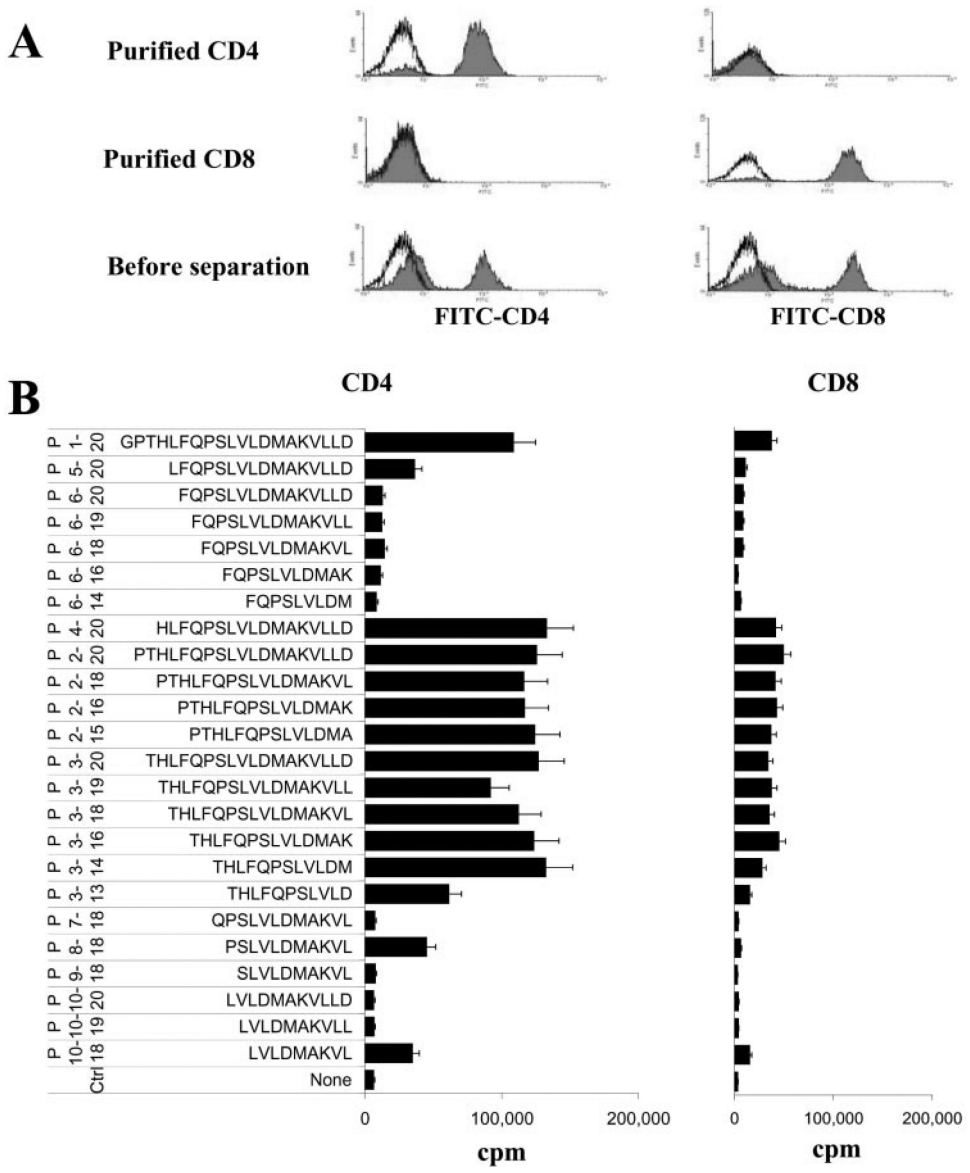

FIGURE 2.

Response of in vivo IRBP1–20-primed T cells to truncated IRBP peptides. *A*, Purity of the CD4 and CD8 T cell preparations. $CD4^+$ and $CD8^+$ T cells were prepared from the spleens of immunized B6 mice 13 days p.i. using StemSep columns (see *Materials and Methods*) and subjected to FACS analysis using FITC-labeled Abs against mouse CD4 or CD8. Controls were stained with FITC conjugate only. Nonfractionated splenic T cells enriched by passage through a nylon wool column are shown in the *bottom panel*. The histogram shows fluorescence on an arbitrary log scale on the *x*-axis. *B*, The proliferative response of purified $CD4^+$ and $CD8^+$ IRBP-specific T cells from IRBP1–20-immunized mice to a panel of truncated IRBP peptides was tested. The results shown are the mean cpm values and are representative of those for five separate experiments, each involving pooled T cells from 8 to 10 IRBP1– 20-immunized B6 mice; the SD was always <15%.

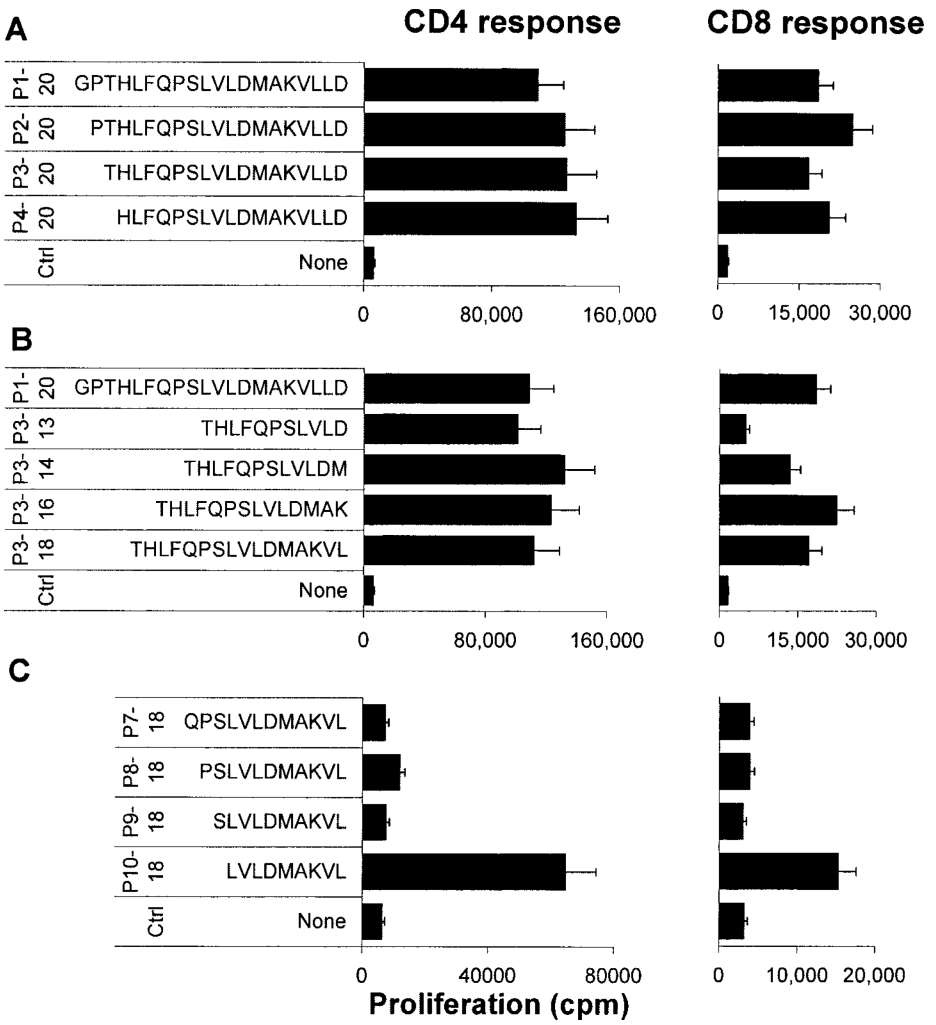

FIGURE 3.

Residues that are crucial for the activation of IRBP1–20-primed T cells in vitro. The proliferative response of purified $CD4^+$ and $CD8^+$ IRBP-specific T cells from IRBP1–20-immunized mice to the indicated IRBP peptides was tested. The results shown are the mean cpm values and are representative of those for three separate experiments, each involving pooled T cells from six to eight IRBP1–20-immunized B6 mice; the SD was always <15%.

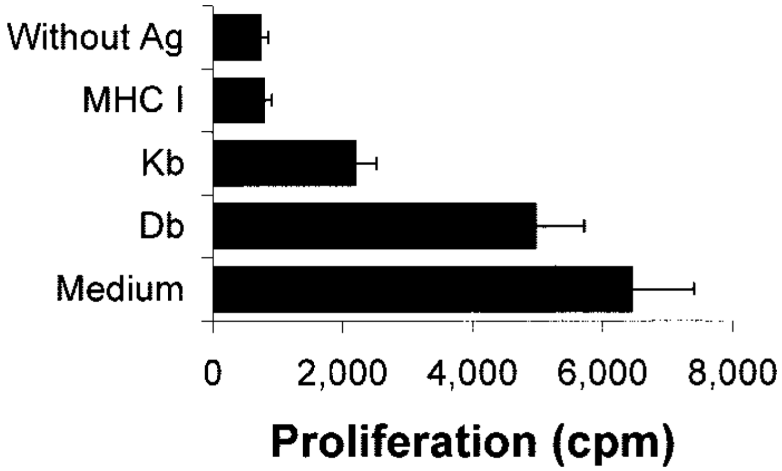

FIGURE 4.

The response of $CD8^+$ IRBP1–20-specific T cells to P10–18 is H-$2D^b/K^b$ restricted. In thymidine incorporation assays, the proliferative response of 4×10^5 in vivo-primed $CD8^+$ IRBP-specific T cells to a suboptimal dose (5 μg/ml) of P10–18 was tested in the absence or presence of Abs against H-$2D^b$, K^b, or both (final concentration 10 μg/ml). The results shown are representative of those for four separate tests.

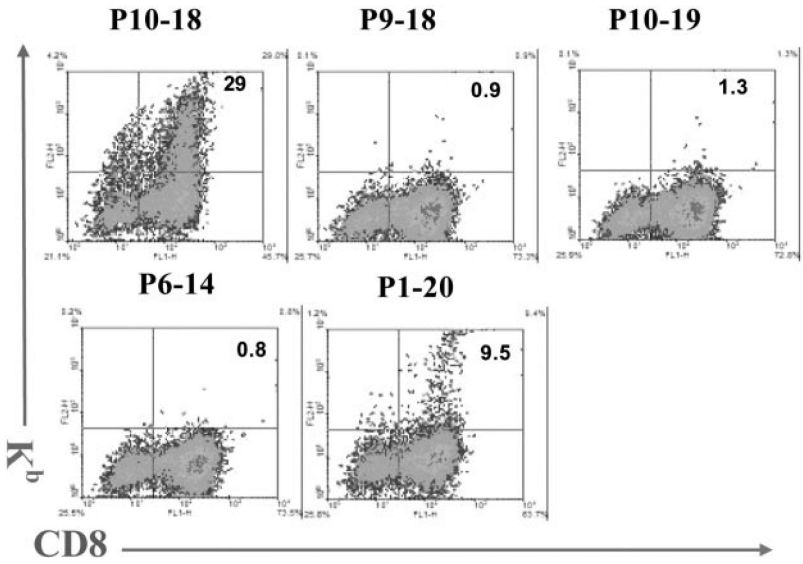

FIGURE 5.

Binding to complexes containing H-2K^b and various IRBP-derived peptides to IRBP1–20-specific T cells. IRBP1–20-specific T cells, prepared from immunized B6 mice 13 days p.i., were stimulated in vitro with 20 μg/ml IRBP1–20 and APCs, then the T cell blasts were separated by Ficoll gradient centrifugation and cultured in IL-2-containing medium for a week. The cells were then incubated with complexes containing H-2K^b and IRBP- peptides (see *Materials and Methods*) (*y*-axis) and FITC-labeled anti-mouse CD8 (*x*-axis).

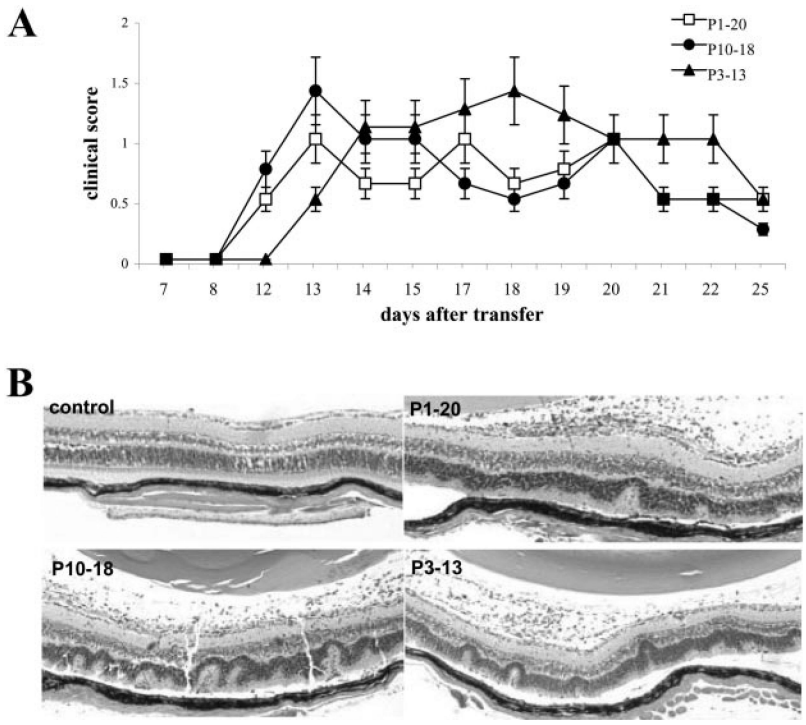

FIGURE 6.

Uveitogenic activity of P10–18- and P3– 13-activated IRBP1–20-specific T cells. Nylon wool-enriched splenic T cells, prepared from IRBP1–20-immunized B6 mice 13 days p.i., were subjected to in vitro stimulation with 20 μg/ml IRBP1–20, P10–18, or P3–13 and APCs, then 5×10^6 T cell blasts, separated by Ficoll gradient centrifugation, were transferred to each recipient mouse. The clinical score was then monitored by fundoscopy, and the eyes of the recipient mice were subjected to pathological examination 15 days later. *A*, Mean clinical score of uveitis after adoptive transfer ($n = 5$). *B*, Eye histology shows that P10–18-and P3–13-stimulated IRBP-specific T cells are potently pathogenic.

Table 1

Truncated peptides derived from IRBP1–20

Peptide	Amino Acid Sequences
IRBP1–20	GPTHLFQPSLVLDMAKVLLD
P2–20	PTHLFQPSLVLDMAKVLLD
P3–20	THLFQPSLVLDMAKVLLD
P4–20	HLFQPSLVLDMAKVLLD
P5–20	LFQPSLVLDMAKVLLD
P6–20	FQPSLVLDMAKVLLD
P6–19	FQPSLVLDMAKVLL
P6–18	FQPSLVLDMAKVL
P6–16	FQPSLVLDMAK
P6–14	FQPSLVLDM
P7–18	QPSLVLDMAKVL
P8–18	PSLVLDMAKVL
P9–18	SLVLDMAKVL
P10–20	LVLDMAKVLLD
P10–19	LVLDMAKVLL
P10–18	LVLDMAKVL
P2–18	PTHLFQPSLVLDMAKVL
P2–16	PTHLFQPSLVLDMAK
P2–15	PTHLFQPSLVLDMA
P3–19	THLFQPSLVLDMAKVLL
P3–18	THLFQPSLVLDMAKVL
P3–16	THLFQPSLVLDMAK
P3–14	THLFQPSLVLDM
P3–13	THLFQPSLVLD